LOCALIZATION OF Na^+-PUMP SITES IN FROG SKIN

JOHN W. MILLS, STEPHEN A. ERNST, and DONALD R. DiBONA

From the Laboratory of Renal Biophysics and Department of Medicine, Massachusetts General Hospital, Boston, Massachusetts 02114, the Departments of Anatomy and Physiology, Harvard Medical School, Boston, Massachusetts 02114, and the Department of Anatomy, Temple University School of Medicine, Philadelphia, Pennsylvania 19140

ABSTRACT

The localization of Na^+-pump sites (Na^+-K^+-ATPase) in the frog skin epithelium was determined by a freeze-dry radioautographic method for identifying [^{3}H]ouabain-binding sites. Ventral pelvic skins of *Rana catesbeiana* were mounted in Ussing chambers and exposed to 10^{-6} M [^{3}H]ouabain for 120 min, washed in ouabain-free Ringer's solution for 60 min, and then processed for radioautography. Ouabain-binding sites were localized on the inward facing (serosal) membranes of all the living cells. Quantitative analysis of grain distribution showed that the overwhelming majority of Na^+-pump sites were localized deep to the outer living cell layer, i.e., in the *stratum spinosum* and *stratum germinativum*. Binding of ouabain was correlated with inhibition of Na^+ transport. Specificity of ouabain binding to Na^+-K^+-ATPase was verified by demonstrating its sensitivity to the concentration of ligands (K^+, ATP) that affect binding of ouabain to the enzyme. Additional studies supported the conclusion that the distribution of bound ouabain reflects the distribution of those pumps involved in the active transepithelial transport of Na^+. After a 30-min exposure to [^{3}H]ouabain, Na^+ transport declined to a level that was significantly less than that in untreated paired controls, and analysis of grain distribution showed that over 90% of the ouabain-binding sites were localized to the inner cell layers. Furthermore, in skins where Na^+ transport had been completely inhibited by exposure to 10^{-5} M ouabain, the grain distribution was identical to that in skins exposed to 10^{-6} M. The results support a model which depicts all the living cell layers functioning as a syncytium with regard to the active transepithelial transport of Na^+.

Since it was first demonstrated that the energy-dependent net transport of Na^+ across the in vitro frog skin was equivalent to the short-circuit current (44), this tissue has been extensively used for studies of active transepithelial Na^+ transport. In fact, the widely accepted conceptual basis for analysis of Na^+ transport across epithelia arose from early studies of this system (25). This scheme depicts Na^+ transport as a two-step process: Na^+ enters an epithelium across an outward facing membrane by passive diffusion down an electrochemical gradient; it is then actively extruded across an inward facing membrane. In epithelia that are composed of only one cell layer the outer and inner barriers can be readily defined, but histological complexity makes localization of these two membranes difficult in the frog skin. Various models which have been pro-

posed in an attempt to define these barriers have conflicted most strongly with regard to localization of the active transport step (8, 12, 19, 25, 45, 47, 49).

Koefoed-Johnsen and Ussing (25) originally proposed a model, based on morphological considerations, that placed the active transport site at the *stratum germinativum,* the innermost cell layer. Later, however, Ussing and Windhager (45) showed, in experiments with microelectrodes, that cells of the *stratum germinativum* could not account for the entire potential measured across the epithelium. From this evidence a new model was proposed that postulated Na^+ pumps in all the living cell layers (45). Na^+ that entered the outermost living cell layer could either be actively extruded into the intercellular space by these same cells or pass, by low resistance intercellular connections, to cells of the other layers and there be actively extruded. Thus, it was proposed that the frog skin might act as a functional syncytium with regard to Na^+ transport.

Recently, a modification of this model has been proposed based on observations of morphological changes in frog skins subjected to short-circuiting, variations in the applied current (47), and application of a serosal hydrostatic pressure head in short-circuited skins (48, 49). Under each of these three conditions the only cells affected were in the outermost living cell layer. These results have led to the hypothesis that the outermost living cell layer is responsible for most of the transepithelial Na^+ transport (49).

A more accurate way to define the Na^+-pump sites in this tissue is to employ a technique that directly visualizes the site of the active transport step. Since the Na^+ pump in most transporting systems, including the frog skin, has been linked to the presence of Na^+-K^+-ATPase (13, 37), localization of this enzyme would more directly identify the site of the Na^+ pump and clarify which, if any, of the many proposed models is correct.

Farquhar and Palade (19) attempted to localize the Na^+ pump in frog skin by employing the procedure of Wachstein and Meisel (50) for the localization of Mg^{++}-ATPase. Their results, which showed the reaction product distributed throughout the different cell layers of the skin, were in essential agreement with the model depicting the Na^+ pump in all the living cells of the epithelium (45). Implicit in the interpretation of results with the procedure of Wachstein and Meisel is the assumption that Mg^{++}-ATPase activity may reflect a different form of the Na^+-K^+-ATPase complex (19). In the light of recent evidence such a view is no longer tenable, because in addition to several kinetic and cytochemical dissimilarities between the two enzymes (14–17), almost all Mg^{++}-ATPase is removed by purification of Na^+-K^+-ATPase (23). Therefore, a definitive localization of the Na^+-pump sites in the frog skin is yet to be accomplished. A plausible working hypothesis depicting the pathway for Na^+ actively transported across the skin depends on the resolution of this problem.

With this in mind, reinvestigation of the site of the Na^+ pump in frog skin was undertaken employing a freeze-dry radioautographic technique for the localization of bound [^{3}H]ouabain (40, 41). Ouabain binds to and inhibits highly purified preparations of Na^+-K^+-ATPase (27) and is also a potent inhibitor of Na^+ transport across the in vitro frog skin (24). [^{3}H]Ouabain is an appropriate marker for a radioautographic approach to the localization of Na^+-pump sites because: its localization can be subjected to rigorous tests of specificity by manipulation of the concentration of ligands that affect its binding to Na^+-K^+-ATPase; it can be bound to the living tissue while monitoring net transepithelial Na^+ transport, thus permitting a correlation of the radioautographic results with the degree of inhibition of the Na^+ pump; and the amount of bound ouabain can be measured by scintillation spectrometry while frequency of binding sites can be determined by analysis of grain distribution. The present study utilizes these features of [^{3}H]ouabain binding to provide a quantitative description of the Na^+-pump distribution in the frog skin. The resulting distribution of binding sites supports consideration of this epithelium as a functional syncytium. Whereas membranes of all the living, noncornified cells participate in the active extrusion of Na^+, most of the ouabain-sensitive Na^+ pumps are in the cells of the *stratum spinosum* and *stratum germinativum.*

MATERIALS AND METHODS

The animals used in this study were female specimens of the bullfrog, *Rana catesbeiana,* (Connecticut Valley Biological Supply, Southampton, Mass.). Frogs were maintained, without feeding, on moistened vegetation at 4°C for up to 2 wk. The Ringer's solution used as tissue bathing medium and as the carrying vehicle for

ouabain had the following composition (in millimolars): Na^+, 110; K, 2; Ca, 1; Mg^{++}, 1; Cl^-, 89; $SO_4^=$, 1; HCO_3, 25. Osmolality was 220–230 mOsm/kg H_2O as determined by freezing-point depression. In experiments with elevated K^+ concentrations, KCl was substituted in equimolar amounts for NaCl. All experiments were carried out at room temperature.

Electrophysiology

To provide adequate control situations, we performed all electrophysiological experiments in Lucite double chambers. Skins from the pelvic region of the animal were mounted as diaphragms oriented so that experimental and control portions were adjacent regions (1 cm^2 in area) from either side of the ventral midline. Initial bathing solutions on both inner and outer surfaces were always the Na^+-Ringer's solution described above. Electrical properties were examined with a square wave voltage clamping routine (9) where transmural potential difference was held alternately at zero (short-circuited state) or 10 mV (inner surface positive to outside) for 10-s intervals. Linearity of the current-voltage relationship over this range permitted a monitoring of transmural conductance by the change in external circuit current with each shift of the clamping voltage. Potential sensing was done with calomel electrodes; current was passed by means of silver-silver chloride electrodes; each was in series with the bathing medium through 3-M KCl-agar bridges. The resulting current trace was plotted on strip chart recorders (model 232, Linear Instruments, Costa Mesa, Calif.). After short-circuit current and conductance had reached stable values (usually by 60 min), ouabain was added to the serosal bathing medium of the designated experimental skin. An equivalent volume of Na^+-Ringer's solution was similarly added to the "control" tissue. Concentrations examined were in the range from 10^{-7} to 10^{-4} M and for periods of 30–180 min. Unlabeled ouabain was obtained from Sigma Chemical Co. (St. Louis, Mo.); the tritiated compound (12 Ci/mM, lot no. 747-186, 170) was from New England Nuclear (Boston, Mass.). The removal of unbound ouabain was done with serial application of a standardized washing procedure that involved draining of serosal chambers and refilling with ouabain-free Na^+-Ringer's solution three times. Washes subsequent to those at the end of the exposure period were performed at 15-min intervals over a 60-min period. Samples for radioautography were then taken as described below.

Ouabain-Binding Studies

Uptake experiments were conducted with [^{3}H]ouabain to determine the minimum exposure time and concentration necessary for saturation of available binding sites. Sheets of ventral pelvic skin were cut into small pieces (4–7 mg wet weight). These were preincubated for 15 min in vials containing standard Na^+-Ringer's solution before the addition of ouabain. In some experiments [^{14}C]inulin (New England Nuclear) was added as a marker for the extracellular space. Pieces of skin in the test solutions were maintained in a shaking water bath at 25°C and gassed with 95% O_2-5% CO_2 for periods of up to 240 min. At predetermined intervals, pieces of skin were removed, blotted, weighed, and processed for liquid scintillation counting. Triplicate samples were taken for determination of binding at each time-point for each animal. In experiments for evaluation of binding in the presence of elevated K^+ concentrations, an identical protocol was followed.

Liquid Scintillation Counting

Pieces of skin, after exposure to [^{3}H]ouabain, were dissolved in measured amounts of NCS reagent (Amersham/Searle Corp., Arlington Heights, Ill.) overnight at 45°C. The next day, after cooling to room temperature, 10 ml of Dimilume-30 (Packard Instruments Co., Inc., Downers Grove, Ill.) was added to 1 ml of the tissue digest, and the ^{3}H concentration was determined in a Nuclear-Chicago Mark I liquid scintillation counter (Amersham/Searle Corp.). Efficiency was measured by the external standard channels-ratio method (peak efficiency for [^{3}H]ouabain of 24%) and the disintegrations per minute per milligram were converted to picomoles of ouabain per milligram wet weight. In dual label experiments, comparing [^{3}H]ouabain to [^{14}C]inulin distribution, isotope concentrations were determined in a Tri-Carb liquid scintillation counter (Packard Instruments Co., Inc.).

Radioautography

[^{3}H]ouabain-treated skins were prepared for radioautography with a method modified from that of Stirling (40). Pieces of skin either cut from chamber-mounted skin specimens or incubated in vials were blotted and quickly frozen by immersion in liquid Freon cooled to liquid nitrogen temperature. Frozen pieces of skin were transferred to a Stumpf-Roth freeze-dry apparatus (Thermovac Industries Corp., Copiague, N. Y.) where one arm containing molecular sieve was at liquid nitrogen temperature and the specimen arm was immersed in an acetone-dry ice bath. Freeze-drying was conducted overnight. The next day the specimen arm was removed from the dry ice bath and allowed to come to room temperature. The side containing molecular sieve was then isolated and the specimen chamber brought to atmospheric pressure with dry nitrogen gas. Osmium tetroxide crystals were quickly placed in the specimen arm, and this side was again evacuated for 5 min by means of a mechanical pump. The osmium crystals rapidly evaporated and this vapor fixation was continued for 1 h. Then the mechanical pump was turned on for 10 min to remove osmium vapors. The specimen chamber was brought to atmosphere with dry nitrogen

gas and the skin specimens were immersed in vials containing Spurr embedding medium (39) which had previously been degassed in a vacuum oven kept at 30 torr. These vials were then quickly transferred to the vacuum oven along with a Petri dish of fresh desiccant (P_2O_5) and the oven was evacuated. Vacuum infiltration was continued overnight before the pieces were embedded in fresh resin. Tissue blocks were cured at 70°C.

Sections ~1 μm thick were cut on glass knives on an Ultratome III (LKB Produkter, Bromma, Sweden), collected on acid-cleaned slides, dipped in NTB-2 emulsion (Eastman Kodak Co.), and stored in light-tight boxes at 4°C for periods of up to 10 wk. Appropriate controls were run simultaneously to rule out chemographic effects. Slides were developed in Dektol (Kodak) for 2 min and stained with a modification of Belanger's method (4), using methylene blue but with the omission of both glycerol and azure A.

Quantitative Analysis of Radioautographic Images

Developed stained slides were examined with a 63× oil immersion objective in a Zeiss light microscope (Carl Zeiss, Ober Kochen, West Germany). Viewed images were directed to a Minicon high resolution video camera (Sierra Scientific Corp., Mountain View, Calif.) and thus transmitted to the display screen of a Princeton 801 Graphics Terminal (Princeton Electronics Products, North Brunswick, N. J.) which permits overlaid displays of video and computer-generated images. The graphics terminal was serially interfaced to a PDP 11/10 computer (Digital Equipment Corp., Maynard, Mass.) and to a "spark-pen" data tablet (Computek, Inc., Cambridge, Mass.). Positional information, e.g., zone boundaries, grain locations, was input through the spark-pen which controlled the movement of an illuminated cursor (or cross hair) superimposed on the terminal display of the image.

The computer program for analysis of grain distribution was designed to assure reasonable objectivity in field selection and in definition of regions within the epithelium. Sections for analysis were chosen as those first obtained from each animal in which tissue preservation was comparable to that obtained with more conventional fixation methods. Field selection (3–8 fields/section) was based on the criteria that all grains could be resolved as individual points and that the skin's outer surface and the basal lamina be parallel since each field was to be divided into rectangular zones.

A sample field and the details of its analysis are shown in Fig. 1. Fig. 1*a* illustrates a radioautograph and the portion of the epithelium that is to be analyzed. Such areas were subdivided into four zones or subpopulations of cells which will be referred to as cornified, granular, spiny, and germinal layers. Cornified and germinal layers correspond to the *S. corneum* and *S. germinativum*, respectively. The granular and spiny designations do not, in every case, refer precisely to the *S. granulosum* and *S. spinosum*, however. Cell position was used as the sole criterion for these designations. The outermost living single layer of cells, just beneath the cornified layer, comprised our granular layer. This corresponds to the reactive cell layer, or RCL, described by Voûte and Ussing (47). The remaining cells between this granular layer and the germinal layer constitute the spiny layer although cells here might include members of both the *S. granulosum* and the *S. spinosum* in a more classical description (7, 18).

The field and zone boundaries were dictated to the program as in Fig. 1*b*. That portion of a viewed field which displayed greatest parallelism of outer surface and basal lamina was delimited with spark-pen selection of top and bottom boundaries (lines A and E). The program then generated additional horizontal lines (B, C, and D) to provide a total of five equidistant vertical references. Each zone boundary was defined with spark-pen selection of an appropriate horizontal coordinate for each of the five reference lines (A–E). The stored description of each zone boundary was a line from top to bottom of the field (connecting A to E) with a horizontal position equal to the mean position of the five selected coordinates for that boundary, e.g., line F at the mean position of points 1 through 5 between spiny and granular layers. In this fashion, grain distribution between zones was based on the position of each grain relative to these mean boundaries. (The effect of this boundary averaging was, as desired, to objectively partition those grains which lay on or near the interfaces between different cell layers.)

Absolute values of grain coordinates were collected by spark-pen identification of the position of each. Recounting was prevented by computer generation of a small square (as in Fig. 1*c*) as it was selected. With storage of both boundary and grain addresses in terms of the coordinate system of the terminal, mathematical analysis of distribution was performed in several modes for each field. Table I summarizes the computer output for analysis of Fig. 1*a*.

In Fig. 1*d*, a graphic representation of the analysis of the field outlined in Fig. 1*b* is presented. Here, grain distribution is plotted as a histogram of frequency vs. depth in the epithelium. The epithelial thickness is divided into 10 equal slices; background estimation is provided by addition of equivalent sampling slices just outside and just inside the epithelium. Consequently, a second "zonal" distribution was obtained for each sample field with normalization to epithelial thickness and apart from a need for subjective distinctions of cell type.

RESULTS

To perform experiments appropriate for subsequent radioautographic analysis, we found it necessary to determine the minimal concentration of

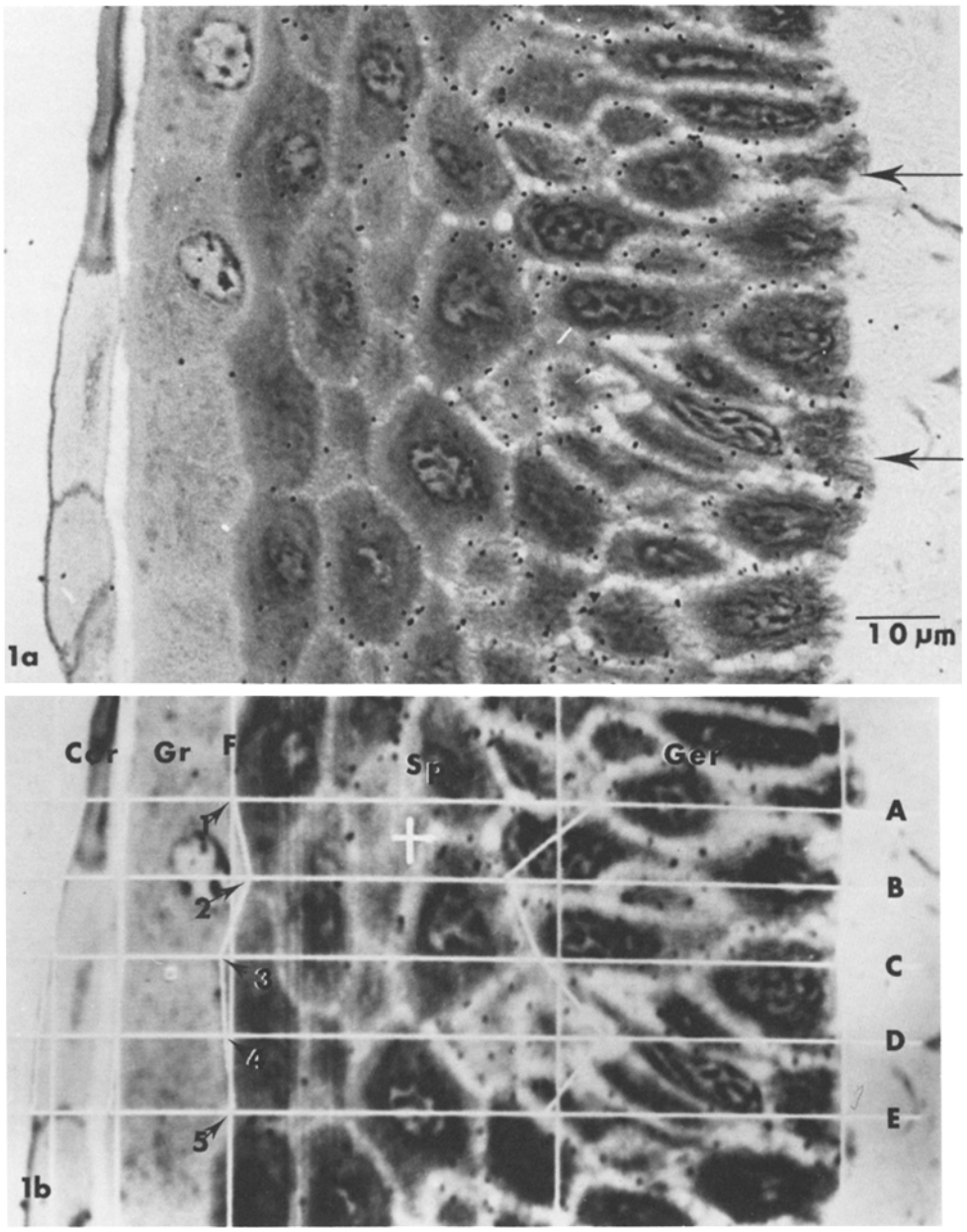

FIGURE 1 An illustration of the method by which radioautographic data was analyzed. (*a*) Sample field from a radioautograph. Area to be analyzed lies between the two arrows. × 1,160. (*b*) Video image of sample field with computer-generated lines superimposed. Vertical straight lines indicate boundaries of different layers. Small square in granular layer (*Gr*) indicates a grain that has been counted. Movement of the cross-bar, seen in the spiny layer (*Sp*), was controlled by a spark-pen and was positioned over each grain to be counted. Ger = germinal layer; Cor = cornified layer.

ouabain that produced a significant reduction in short-circuit current (SCC) within a reasonable time period and to determine whether [^{3}H]ouabain binding saturated with time. These precautions were necessary in order to eliminate any nonspecific binding that might occur with the

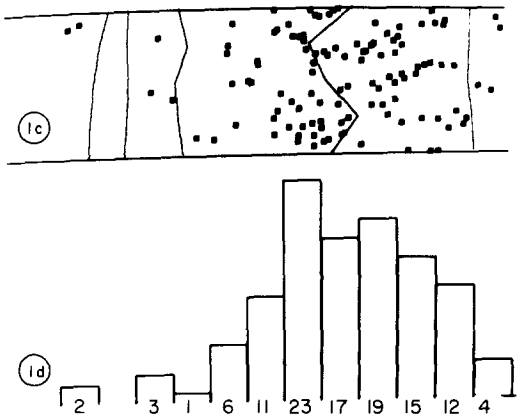

FIGURE 1 (*c*) Computer output showing the grain distribution within the boundaries defined in Fig. 1 *b* after all the grains had been counted. The position of individual squares is based on coordinates input by spark-pen identification of each grain. (*d*) The grains contained within the boundaries of Fig. 1 *b* plotted as a histogram of frequency vs. depth in the epithelium. The epithelial thickness is divided into 10 slices of equal cross-sectional area. Numbers below each bar are the numbers of grains in each slice. The absence of a bar at the second position in from the left indicates that there were no grains in that slice. The first and last bar indicate grains in slices, each equal to 10% of the epithelial thickness, used to estimate background. Figs. 1 *b*, *c*, and *d* can be superimposed to show the region of greatest grain density.

use of relatively high concentrations of ouabain (3) and to insure that all binding sites were reached to allow an accurate radioautographic localization. As shown in Fig. 2, inhibition of SCC across the frog skin is strongly dose dependent. Concentrations at 10^{-6} M and above caused a substantial drop in SCC within 120 min.

[^{3}H]Ouabain Uptake vs. Concentration

Analyses of uptake at different concentrations of ouabain demonstrated a saturable component at low concentrations and a nonsaturable component at ouabain concentrations above 10^{-5} M (Fig. 3). This is in agreement with the results of Baker and Willis (3) and Brading and Widdicombe (5). On the basis of this result, and those in Fig. 2, a concentration of 10^{-6} M was selected (the actual range was 1.2–1.6 × 10^{-6} M). This concentration satisfied the criterion for effective inhibition of SCC within a time period where the spontaneous decline of current in the control was not a substantial factor. It was also below the concentration level where a large proportion of the binding of ouabain could be attributed to a nonsaturable component.

To determine an adequate rinse period to remove unbound [^{3}H]ouabain, a necessary prerequisite for accurate radioautographic localization, we constructed a washout curve using [^{14}C]inulin as a marker to determine the time necessary to remove an unbound molecule from the extracellular space (Fig. 4). In these experiments pieces of frog skin were incubated for 120 min in Na^+-Ringer's solution containing [^{14}C]inulin. Then the incubation fluid was replaced at specified intervals by equal volumes of inulin-free Ringer's solution for a total period of 120 min. After 30 min of wash time, 90% of the inulin originally in the tissue was removed and after 60 min, 93% was removed. An additional 60 min of wash removed only 2% more of the marker (95% of the inulin washed out). Therefore, in all subsequent experiments to determine the amount of bound ouabain (vs. total uptake) or to use the tissue for radioautography, the skin was subjected to a 60-min wash period in ouabain-free medium.

Effect on Na^+ Transport

The time-course of the effect of 10^{-6} M ouabain on SCC across the frog skin is shown in Fig. 5 A. After a substantial lag period (30 min) a sharp reduction in SCC is evident. Fig. 5 A demonstrates that this inhibition of SCC in the frog skin is not reversible. As was found for the frog bladder (32), SCC does not show any sign of returning to control levels even after extensive washings of the skin with ouabain-free medium. At the end of this 180-min incubation-wash period the skin had bound 0.475 pmol ouabain/mg (Table II). The conductance showed a less rapid decline than the SCC but was still significantly reduced ($P < 0.02$) after the 120-min exposure to ouabain (Fig. 5 B). Like the SCC, the conductance continued to decline even after extensive washes to remove ouabain. Ouabain also caused a significant reduction (64%) in the calculated potential difference over the 120-min exposure period (Fig. 5 C). After the wash period was begun, the decline in potential was halted but there was no sign of recovery.

Specificity of Binding

Since nonspecific ouabain binding might occur simultaneously with the saturable component of interest (35) it was necessary to test further for the degree of specificity at 10^{-6} M. The reduction in the binding achieved by increasing the K^+ con-

centration in the incubation medium has been interpreted as indicating the degree of specific binding both in biochemical assays and in intact cell preparations (3, 31, 32, 34, 42). However, it has been shown that the effect of K^+ on ouabain binding to Na^+-K^+-ATPase preparations is on the rate of the ouabain-enzyme interaction (1, 29, 36). Consequently, the length of the exposure to ouabain in Ringer's solutions containing various K^+ concentrations is critical to the interpretation of the degree of specific vs. nonspecific binding.

These considerations led to a detailed analysis of the time-course of ouabain binding to the frog skin and its response to variations in the medium

TABLE I

Analysis of Grain Distribution in Figure 1 a

Layer	Grains	Total grains	Density*
		%	
Outside skin	2	1.77	0.41
Cornified	0	0	0
Granular	3	2.65	0.44
Spiny	48	42.49	2.37
Germinal	56	49.56	3.22
Inside	4	3.53	0.83
Total	113	100.00	
Mean density			2.26

* Density given in terms of graphics terminal coordinates.

K^+ concentration. As shown in Fig. 6, binding of ouabain to skins incubated in standard Na^+-Ringer's solutions reached an equilibrium value by ~120 min. By comparison, inulin reached equilibrium within the extracellular space by 90 min (data not shown). The amount of bound ouabain at 120 min was 93% of that after 240 min of incubation. Binding of ouabain to frog skin in the presence of 42 mM K^+-Ringer's solution was unaltered at the earliest time-point (15 min) but was significantly reduced at 30, 60, and 90 min ($P < 0.05$). The mean values for the tissue binding in 42 mM K^+ solutions at 120, 180, and 240 min were slightly but not significantly lower ($P > 0.05$) than in Na^+-Ringer's solutions. Also plotted in Fig. 6 are the mean values for two experiments in which uptake was measured in an 85 mM K^+-Ringer's solution. For the first 120 min these points are indistinguishable from those obtained with uptake in 42 mM K^+. It is evident, therefore, that the maximal effect on ouabain binding was achieved by the lower K^+ concentration.

It is possible that the high K^+ solutions had caused a significant degree of cell swelling (46). In that case some of the differences in binding shown in Fig. 6 could have been due to the inability of ouabain to freely diffuse to all its receptor sites. (Correcting for inulin space would not eliminate this problem since it does not correct for the possible blockage of ouabain from reach-

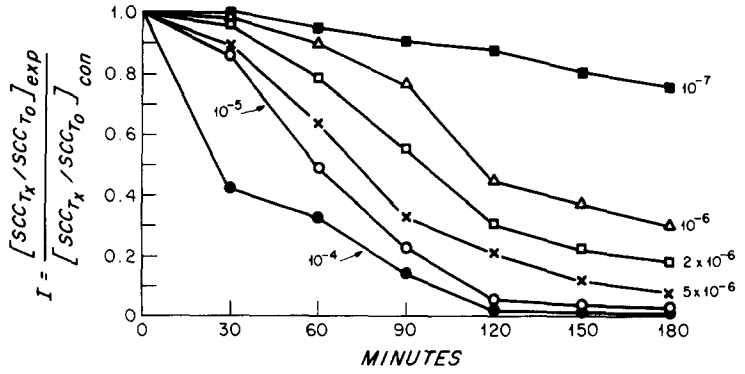

FIGURE 2 Effect of different concentrations of ouabain on SSC across the frog skin. The ordinate is the fractional change in SCC normalized for spontaneous variations with time in the paired control skin by the equation

$$I = (SCC_{T_x}/SCC_{T_0})\ \text{exp}/(SCC_{T_x}/SCC_{T_0})\ \text{con}$$

where T_0 is the SCC value just before addition of ouabain and T_x is the SCC at the designated time intervals. The points for each line are the means from two experiments.

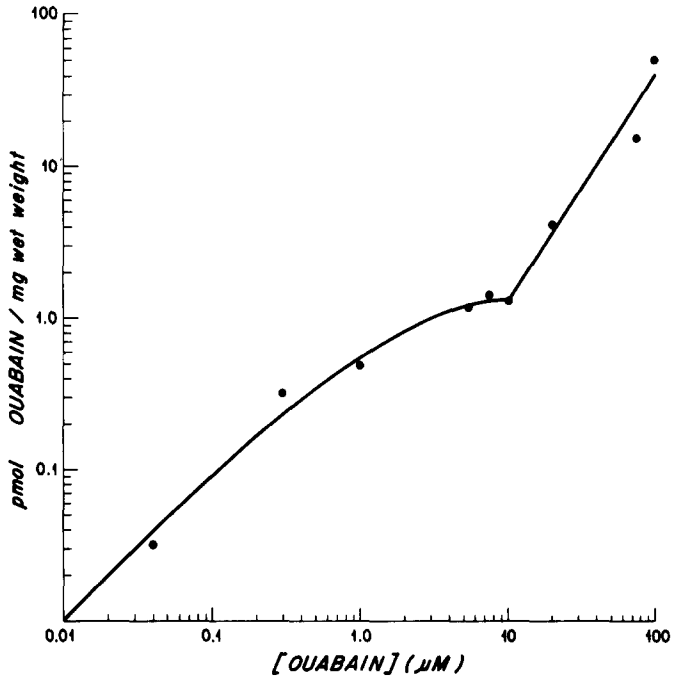

FIGURE 3 Uptake of ouabain into unwashed pieces of frog skin at different concentrations. Values are corrected for extracellular label by subtracting ouabain distributed in simultaneously determined inulin space. Pieces of skin (4–7 mg wet weight) were exposed to ouabain for 120 min. The curve was fitted by eye. Note that both the abscissa and ordinate are on a log scale. Each point is the mean from determinations on three to six animals.

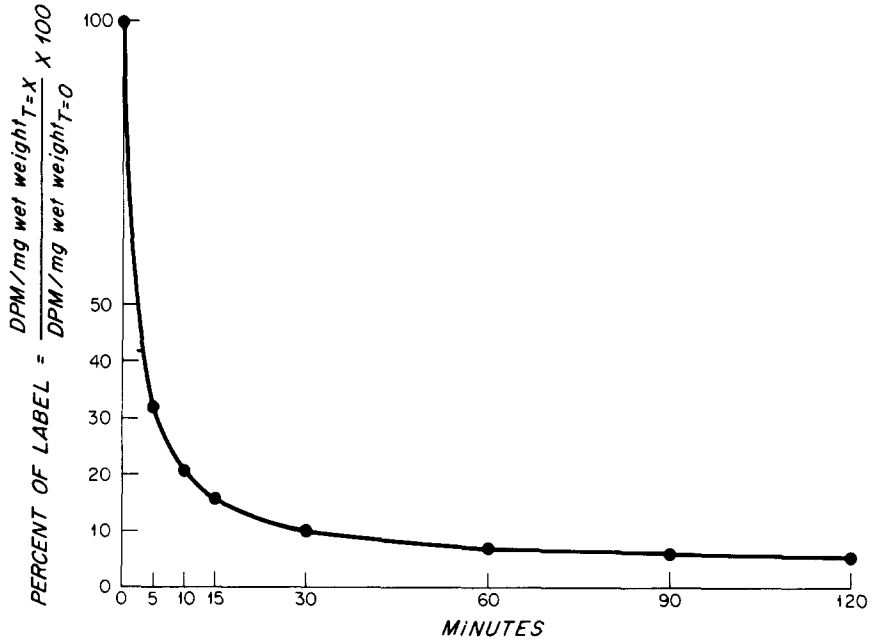

FIGURE 4 Washout time for [^{14}C]inulin in the frog skin. Pieces of skin were exposed to [^{14}C]inulin in Na^+-Ringer's solution for 120 min. Then the incubation solution was replaced by inulin-free Ringer's solution at time zero. Solutions were changed again at each time marked. All washes were saved and the amount of inulin in the washes was added to the amount remaining in the tissue after 120 min of wash time to determine the value for zero time. The results are then reported as the amount of label in the tissue plus wash solution at each subsequent time-point expressed as a percent of the value at time zero.

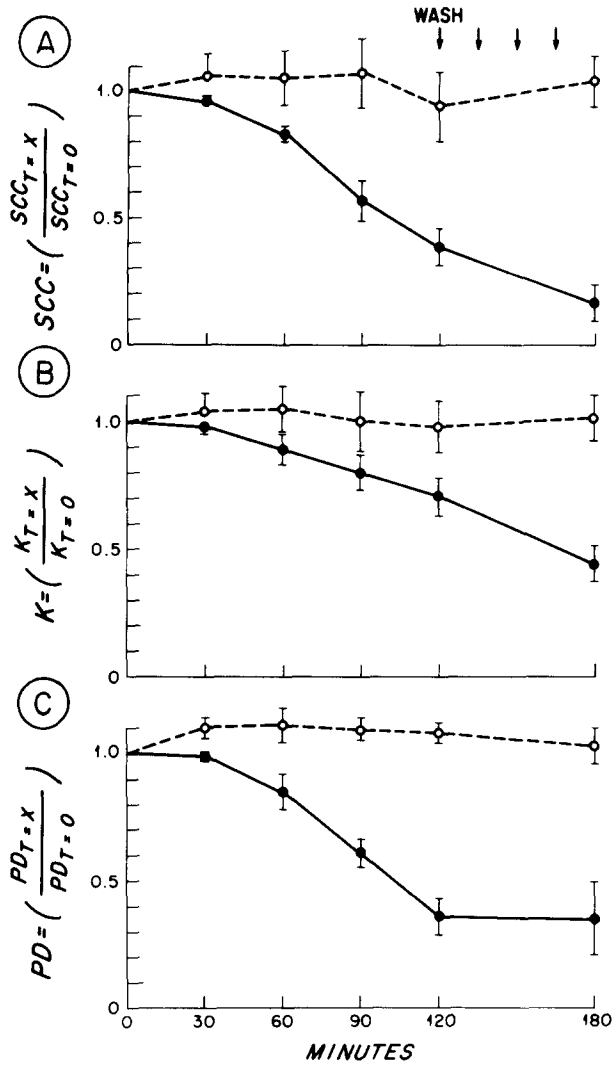

FIGURE 5 Effect of ouabain (1.2–1.6 × 10^{-6} M) on SCC, conductance (*K*), and potential difference (*PD*) across the frog skin. The ordinate is expressed as the fractional change in each parameter in relation to time zero. Ouabain was added to the serosal solution of the experimental side at time zero (solid circles). The control received an equal amount of Na^+-Ringer's solution (open circles). Arrows indicate when the serosal chambers were drained and refilled with ouabain-free Ringer's solution. (N = 7) ± SEM. (A) Effect on SCC. (B) Effect on conductance (*K*). (C) Effect on PD.

ing the outer cell layers through closed intercellular spaces.) Swelling was not evident in our frog skin preparations exposed to high K^+-concentrations; there was no significant difference in the amount of extracellular water/milligram wet weight in skins exposed to 42 mM K^+-Ringer's solution compared to those exposed to Na^+-Ringer's solution.

The data in Fig. 6 were analyzed by a double reciprocal plot. This procedure gives values for the equilibrium binding point (Y-intercept) and the half-maximal load time (X-intercept). For Na^+-Ringer's solution with 10^{-6} M ouabain, the half-maximal load time was 28.3 ± 3.5 min and the equilibrium binding value was 0.677 ± 0.022 pmol/mg wet weight. For 42 mM K^+-Ringer's solution, the corresponding values were 54.6 ± 17.3 min and 0.653 ± 0.071 pmol/mg wet weight (Fig. 7). Further evidence that K^+ affects the rate of the ouabain-receptor interaction is pro-

TABLE II

Binding of [^{3}H]Ouabain to Frog Skin

Conditions*	pmol Ouabain/mg wet weight	
120-min Exposure to 10^{-6} M ouabain under short-circuit conditions (7)	0.475 ± 0.035	
ATP Depletion		
Control‡ (4)	0.308 ± 0.046	
Anoxic (4)	0.140 ± 0.006	
Binding in Na-R vs. 42 K-R§	Na-R	42 K-R
30 min (4)	0.320 ± 0.033	0.133 ± 0.014
60 min (4)	0.382 ± 0.033	0.217 ± 0.022
90 min (4)	0.479 ± 0.045	0.299 ± 0.035
30-min exposure followed by incubation in ouabain-free Ringer's (5)	0.224 ± 0.030	
10^{-5} M ouabain, time of exposure necessary to reduce SCC to zero (4)	0.809 ± 0.125	

* All tissue subjected to 60-min wash period in ouabain-free Ringer's solution before determination of ouabain binding.

‡ Exposed to anoxic period, then re-exposed to air before addition of [^{3}H]ouabain.

§ Na-R is standard Na^+-Ringer's solution; K-R is Ringer's solution containing 42 mM K^+.

Numbers in parentheses are the numbers of animals used.

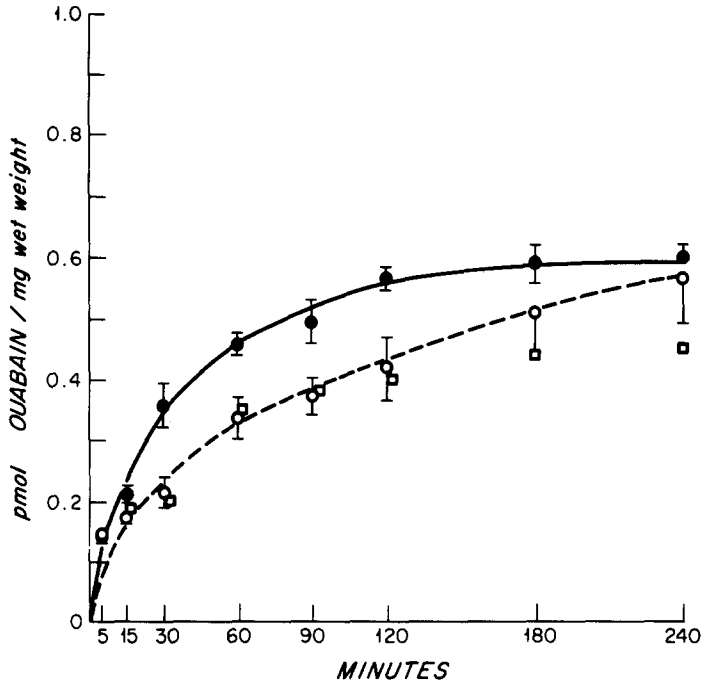

FIGURE 6 "Tissue binding" of ouabain to frog skins bathed in Na^+-Ringer's (closed circles) or 42 mM K^+-Ringer's solution (open circles). Ouabain concentration was 10^{-6} M. Skins were prepared for liquid scintillation counting without prior washing in ouabain-free Ringer's solutions. Points for this graph were determined by subtracting the amount of ouabain in the simultaneously determined inulin space from the total ouabain uptake (N = 5) ± SEM. Squares indicate tissue binding in skins incubated in 85 mM K^+-Ringer's solution. (N = 2).

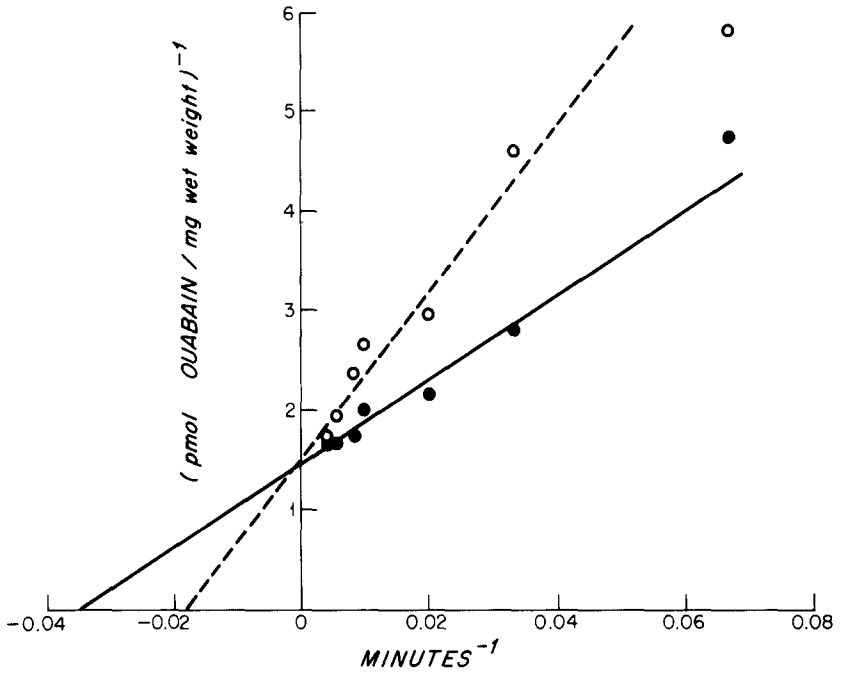

FIGURE 7 Double reciprocal plots of the data used to construct Fig. 6. The 5-min points, although not shown here, were used to determine the equations of the lines as drawn. The lines were drawn according to the equations generated by the computer program of Cleland (10). Symbols are the same as in Fig. 6. The Y-intercept is equal to the reciprocal of the maximal amount bound. The X-intercept is equal to minus the reciprocal of the half-maximal uptake time. Although the binding of ouabain to Na^+-K^+-ATPase is a bimolecular reaction and follows, therefore, second-order kinetics, <1% of the ouabain in the media was taken up by the tissue during the incubation period. Accordingly, the kinetics approximate first order and the constants determined by a double reciprocal plot are empirically accurate.

vided by electrophysiological experiments (Fig. 8). The reduction in SCC in skins exposed to ouabain with a 42 mM K^+-Ringer's solution on the serosal side was significantly less than in paired controls exposed to ouabain in Na^+-Ringer's solution ($P < 0.05$). In addition, the slope of the decline was reduced.

A ligand necessary for binding of ouabain to Na^+-K^+-ATPase preparations is ATP (30, 31, 42). In biochemical assays of the specificity of binding to the enzyme it is relatively easy to alter the ATP concentration. In intact cells, however, this is a more difficult problem. Previously, it was shown that binding of ouabain to the frog urinary bladder was greatly reduced by subjecting the bladder to an anoxic period and then conducting the binding experiment in the anoxic environment (32). An anoxic period of 40 min has been shown to reduce the ATP level in the toad bladder by 30% (21). Similar results have been reported for the frog skin where it was found that incubation under anaerobic conditions reduced the ATP/ADP ratio (26). Therefore, we conducted binding experiments in skin subjected to an anoxic environment by bubbling N_2 gas through the Na^+-Ringer's[1] in the chamber. The control skin was also subjected to an anoxic period and then air was bubbled into the chamber and a new steady state was achieved before the addition of ouabain. Both the control and experimental sides were exposed to ouabain for 120 min followed by a 60-min wash period. Skins exposed to an anoxic environment throughout the experiment bound 0.140 ± 0.006 pmol/mg wet weight (Table II). This is in comparison to 0.308 ± 0.046 pmol/mg wet weight bound to the reoxygenated controls.

[1] For these experiments the Na^+-Ringer's solution had the following composition (in millimolars): Na^+, 113; K^+, 3.6; Ca^{++}, 0.9; Cl^-, 114.8; $HPO_4^=$, 1.7; $H_2PO_4^-$, 0.2.

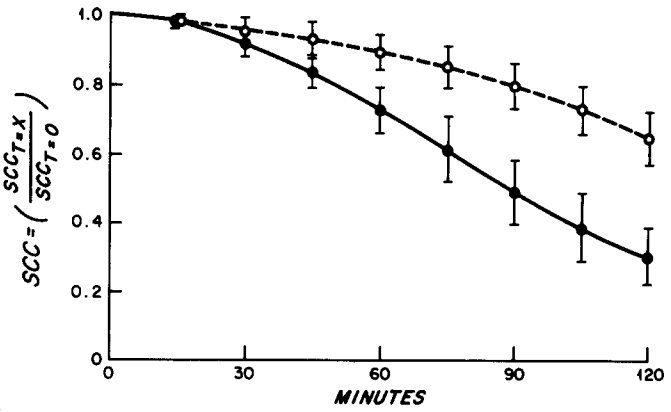

FIGURE 8 Effect of ouabain (10^{-6} M) on SCC across frog skins incubated in Ringer's solutions. Skins had either Na^+-Ringer's on both the mucosal and serosal sides (closed circles) or Na^+-Ringer's on the mucosal side and 42 mM K^+-Ringer's on the serosal side (open circles). Skins were exposed to the respective Ringer's solutions and a steady state was achieved before the addition of ouabain at time zero. Notice that the decline in SCC is not so rapid in the K^+-treated skins as in skins exposed to ouabain with Na^+-Ringer's on both sides. (N = 4) ± SEM.

Radioautography: Distribution of Ouabain-Binding Sites[2]

Fig. 9 provides an example of grain distribution in skins exposed to [^{3}H]ouabain (10^{-6} M) for 120 min and then washed for 60 min in ouabain-free medium. The localization of grains over intercellular spaces reflects ouabain bound to plasma membranes. All of the noncornified cells are labeled with the heaviest concentration of grains seen in the inner portion of the spiny layer. Cells of the germinal layer are also heavily labeled. In the transitional area between the cells of the spiny and granular layers there is a sharp drop-off in grain density. The granular, or outermost living cell layer, consistently showed less evidence of bound ouabain than the deeper cell layers. Mitochondria-rich cells (Fig. 9) were less labeled than the surrounding epithelial cells. The cornified cells did not exhibit a degree of labeling above that of the background, nor did the outward facing membrane of the first living cell layer.

Computer analysis of grain distribution in skins exposed to ouabain, as in Fig. 9, showed that 41% of the grains were located in the spiny layer (Fig. 10 A). In addition, 39% of the grains were in the germinal layer. The granular layer (the outer living cell layer) had 13.2% of the grains. The remaining 6.8% were distributed over the cornified layer and the two areas on each side of the skin used to assess background. These results show that both the spiny layer and the germinal layer have at least three times as many ouabain-binding sites as the granular layer. However, since the layers, as we have defined them, do not constitute equivalent areas, a comparison of grain density between regions is not provided by this mode of analysis.

This problem was examined by computer division of each examined field into 10 slices of equal cross-sectional area and categorization of grain position with respect to these slices (see Materials and Methods and especially Fig. 1 *d*). The cumulative results of this density analysis are expressed as a histogram (Fig. 11). The spiny layer, represented by slices 5, 6, and 7, had the highest density of grains. Slices 2 and 3, which would include all of the granular layer, had a density that was similar to that in the germinal layer (slices 9 and 10). It also should be noted that the grain density in slice 2, located between 10 and 20% of the epithelial thickness from the outer edge of the epithelium, is significantly less than the density in slice 3 ($P < 0.01$). Thus, the resulting density distribution describes a dramatic increase in binding sites with distance progressively farther from the first living cell layer. The density in slice 1, the cornified layer, was not significantly different from background. These results demonstrate that the visual impression gained from Figure 9, that the inner cell layers have the greatest number of pump

[2] The terminology used here and in the figure legends corresponds to that defined in Materials and Methods.

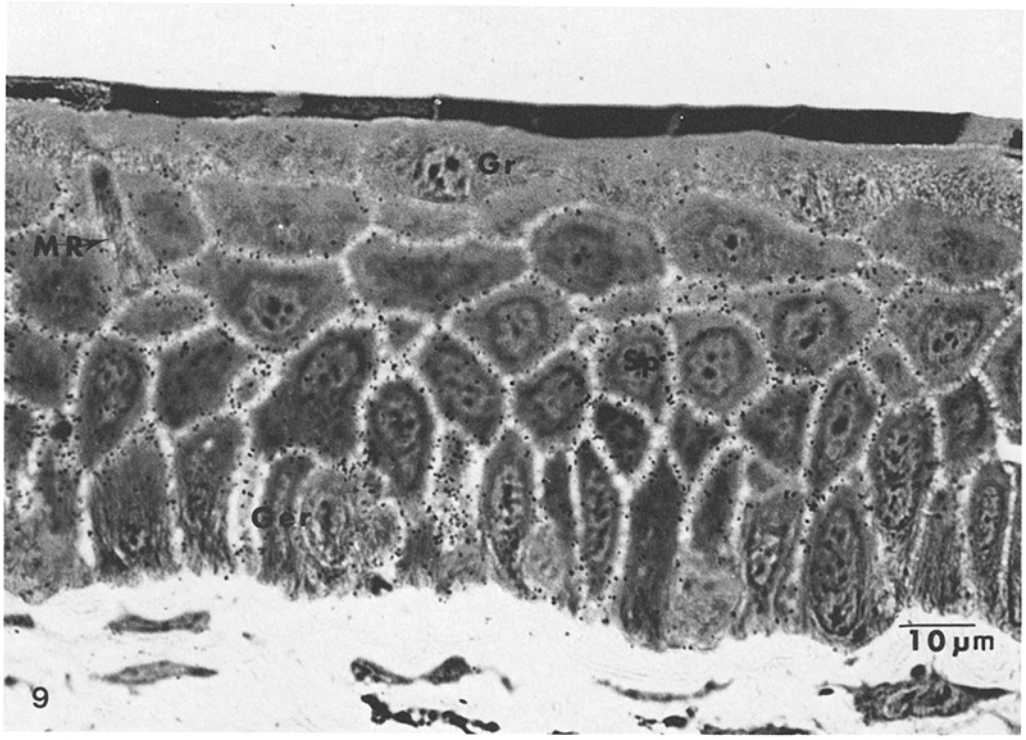

FIGURE 9 Radioautograph of frog skin exposed to 10^{-6} M [^{3}H]ouabain for 120 min followed by a 60-min wash period in ouabain-free Na^+-Ringer's. Grains, indicating [^{3}H]ouabain-binding sites, are distributed throughout the epithelium. The heaviest concentration of grains is in the spiny layer (Sp). M-R = mitochondria-rich cell, Ger = germinal layer, Gr = granular layer. × 1,088.

sites, is substantiated by quantitative analysis of the grain distribution. It should be emphasized, nonetheless, that the number of grains associated with each living cell layer (slices 2-10) was significantly greater than background ($P < 0.01$). Although there is an uneven distribution of grains, all the living cells possess ouabain-binding sites.

The relevance of any analysis of grain distribution depends on the assumption that ouabain reaches all the available binding sites. Analysis of binding vs. time and concentration showed that ouabain uptake follows saturation kinetics. The implication that saturation reflected the ability of ouabain to reach all potential binding sites was confirmed by radioautography (Fig. 12). In this view of a piece of skin, which was incubated for 90 min in a Na^+-Ringer's solution containing [^{3}H]ouabain and then frozen without being subjected to a wash period, [^{3}H]ouabain has diffused throughout the epithelium. It is also important to note that ouabain is excluded from the interior of the living cells but penetrates the dead cells of the cornified layer.

The localization of binding sites in Fig. 10 is typical for skins exposed to 10^{-6} M ouabain for 120 min. However, it is important to emphasize that there was occasionally a large variation in the observed grain distribution. This was true between samples from the same animal as well as between different animals. This variation is depicted in Fig. 13 where the grain distribution between cells in a single sample is quite dramatic. In one area of the epithelium the grains are predominantly localized to the germinal layer while in an adjacent area the distribution is centered in the spiny layer. The variations observed were usually between these two layers. In only one of the 31 animals analyzed in the radioautographic portion of this study was the grain density in the granular, or outer living cell layer, greater than in the spiny layer.

Since it is a fair assumption that all cells have Na^+-K^+-ATPase, ouabain-binding sites in the

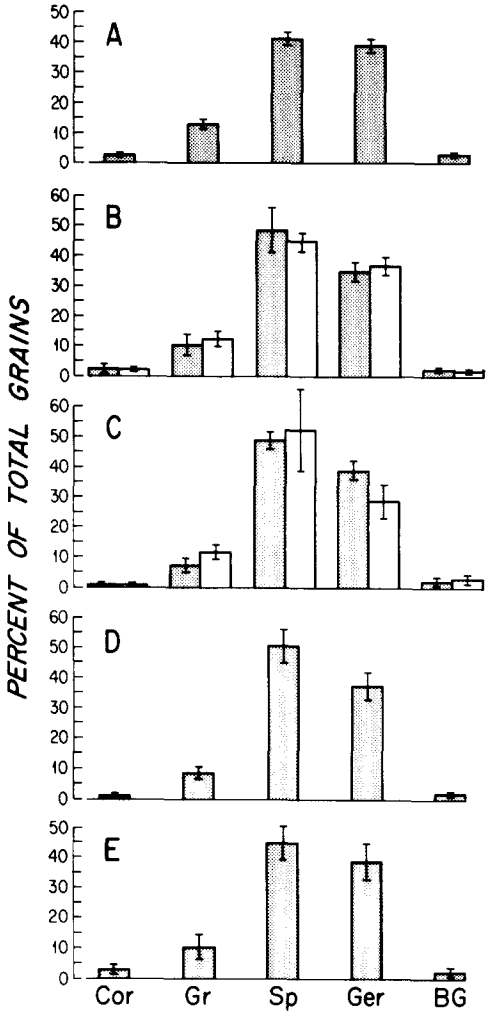

FIGURE 10 Grain distribution in the different layers of the frog skin expressed as the percent of the total grains counted. Cor = cornified layer, Gr = granular layer (outer living cell layer), Sp = spiny layer, Ger = germinal layer, BG = background grains (mean ± SE). (A) Skins exposed to 10^{-6} M [^{3}H]ouabain for 120 min followed by a 60-min wash period (N = 7). (B) Skins exposed to 10^{-6} M [^{3}H]ouabain for 30 min in Na^+-Ringer's (hatched bars) or 42 mM K^+-Ringer's (open bars) solutions followed by a 60-min wash. None of the differences between paired values were significant. (N = 4). (C) The distribution in skins continuously incubated under anoxic conditions (open bars) compared to the distribution in skins that were reexposed to air (hatched bars) before the addition of 10^{-6} M [^{3}H]ouabain. Exposure to ouabain was conducted for 120 min followed by a 60-min wash period (N = 4). (D) Skins exposed to 10^{-6} M [^{3}H]ouabain for 30 min, followed by a rapid washout, and then a continued incubation in ouabain-free Ringer's solution (N = 4). (E) Skins exposed to 10^{-5} M [^{3}H]ouabain until the SCC reached zero, followed by the standard wash procedure (N = 4).

spiny layer (or for that matter, any layer) are not necessarily important sites for the transepithelial transport of Na^+. However, with the protocol used in this study, other cells in the skin which are not part of the epithelium, such as pigment cells and fibroblasts, did not show a grain localization that was above background. Also, as shown in Fig. 14, epithelial cells lining the neck of a gland do not show an appreciable number of binding sites, especially when compared to the epithelial cells in the adjacent layers of the skin.

Radioautography: Specificity of Ouabain Binding

The effect of ligand concentrations on the distribution of ouabain-binding sites was examined by radioautography. Based on the data in Figs. 6 and 7, radioautographic analysis of specific binding sites was determined on skins exposed to ouabain in Na^+-Ringer's or 42 mM K^+-Ringer's for 30, 60, and 90 min. Grain counts were greatly reduced in radioautographs of skins incubated in 42 mM K^+-Ringer's solution when compared to paired samples incubated in a standard Na^+-Ringer's solution (Fig. 15). The reduction in grains throughout the epithelium is obvious. These pieces of skins were exposed to [^{3}H]ouabain for 30 min, an incubation period expected to result in only half of the maximal binding (Fig. 6). Yet, at this time a number of the grains are located in the granular layer (Fig. 15*a*), indicating that ouabain diffused throughout the epithelium within this time period. Although ouabain binding in a high K^+ concentration was significantly reduced (Table II), computer analysis showed that the relative grain distribution was unchanged, indicating that binding in each layer was equally affected (Fig. 10B). The results at 60 and 90 min were similar to those shown for 30 min. These radioautographs (Fig. 15) also demonstrate that there is no detectable swelling of the epithelial cells after incubation in 42 mM K^+-Ringer's solution.

Analysis of the grain distribution was also conducted in skins exposed to an anoxic period, in order to reduce ATP levels. Fig. 10C shows that,

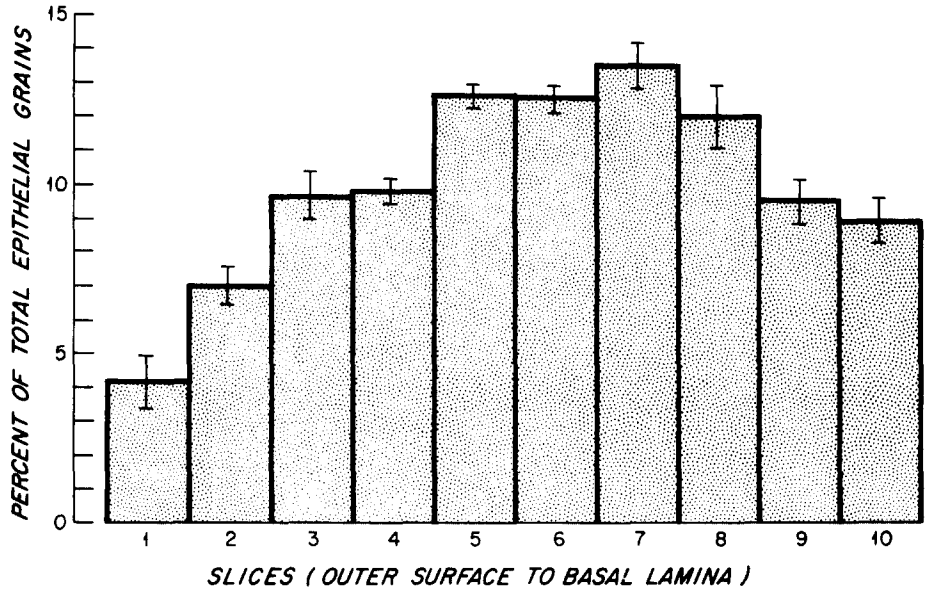

FIGURE 11 Distribution of grains in the frog skin represented as the percentage of grains in 10 slices of equal cross-sectional area. Slice 1 begins at the outer border of the corneum, and slice 10 ends at the base of the germinal layer. Skins same as in Fig. 10 A (N = 7).

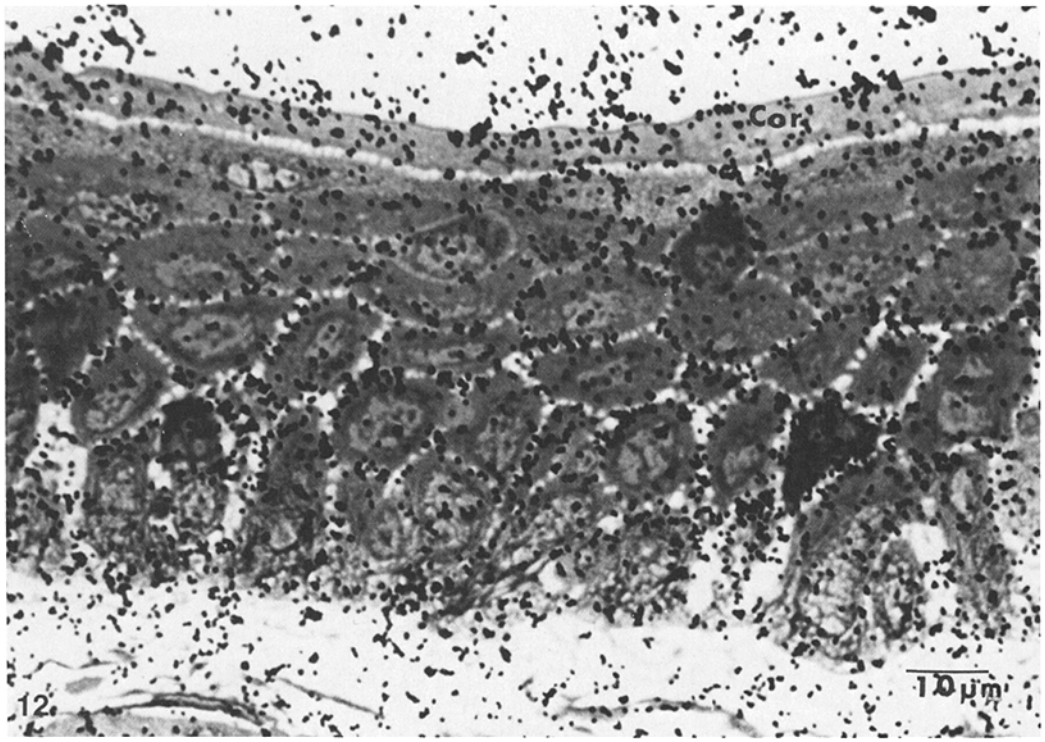

FIGURE 12 Radioautograph of skin incubated in 10^{-6} M [^{3}H]ouabain for 90 min. Skin frozen without wash period to remove unbound label. Grains are distributed throughout the intercellular spaces of the epithelium. There is no significant penetration of ouabain into cells except in the cornified layer (*Cor*). Exposed for 28 days. × 1,160.

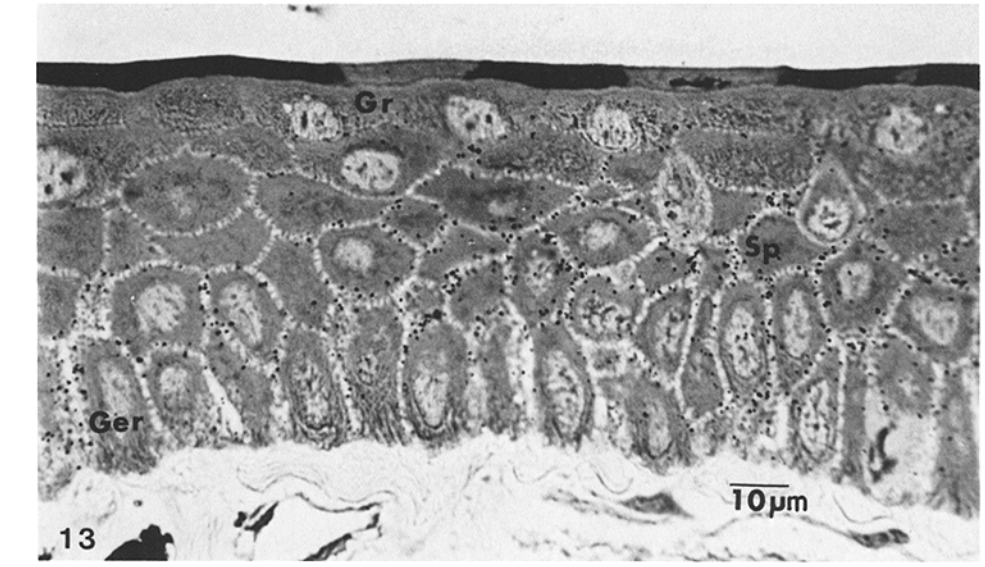

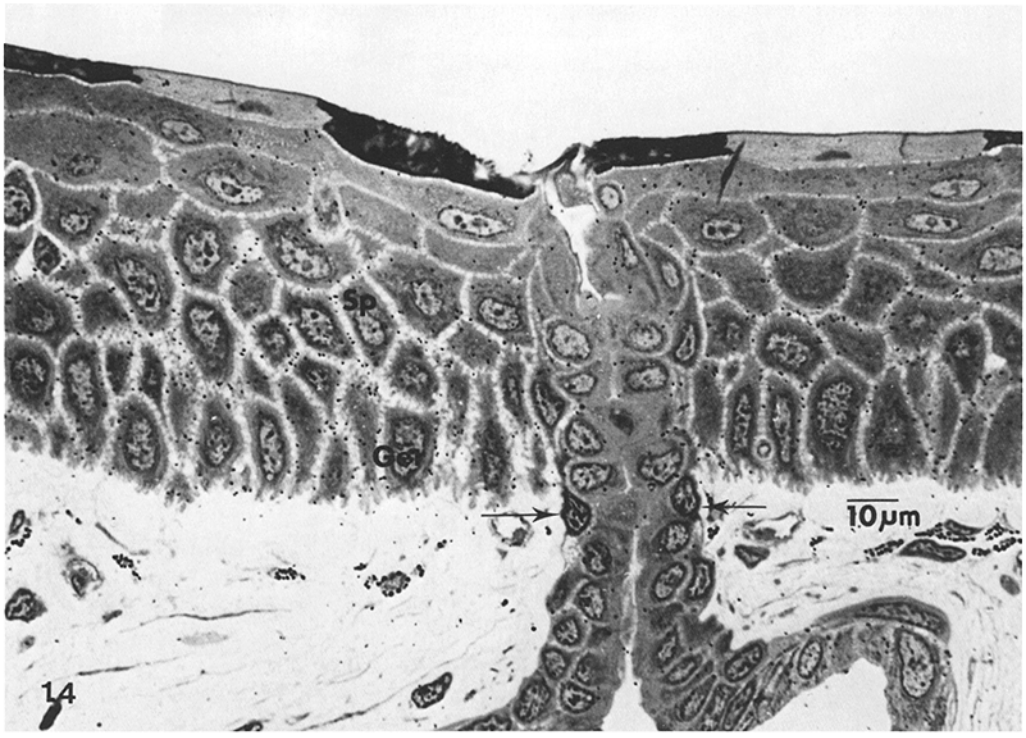

FIGURE 13 Radioautograph of frog skin incubated with 10^{-6} M [^{3}H]ouabain for 120 min followed by a 60-min wash in ouabain-free Na^+-Ringer's. On the left side of the figure the grains are predominantly localized to the germinal layer (*Ger*) and the transitional zone between the germinal and spiny layers (*Sp*). In the field to the right the grains are predominantly localized to the spiny layer, with fewer grains associated with the germinal layer. The granular layer (*Gr*) has almost no grains associated with it. 14-day exposure. × 736.

FIGURE 14 Radioautograph of skin incubated with 10^{-6} M [^{3}H]ouabain for 120 min followed by a 60-min wash in ouabain-free Na^+-Ringer's. Binding sites associated with the neck of a gland (arrows) are few, especially in comparison to the localization seen in the adjacent cells of the spiny (*Sp*) and germinal (*Ger*) layers. 14-day exposure. × 690.

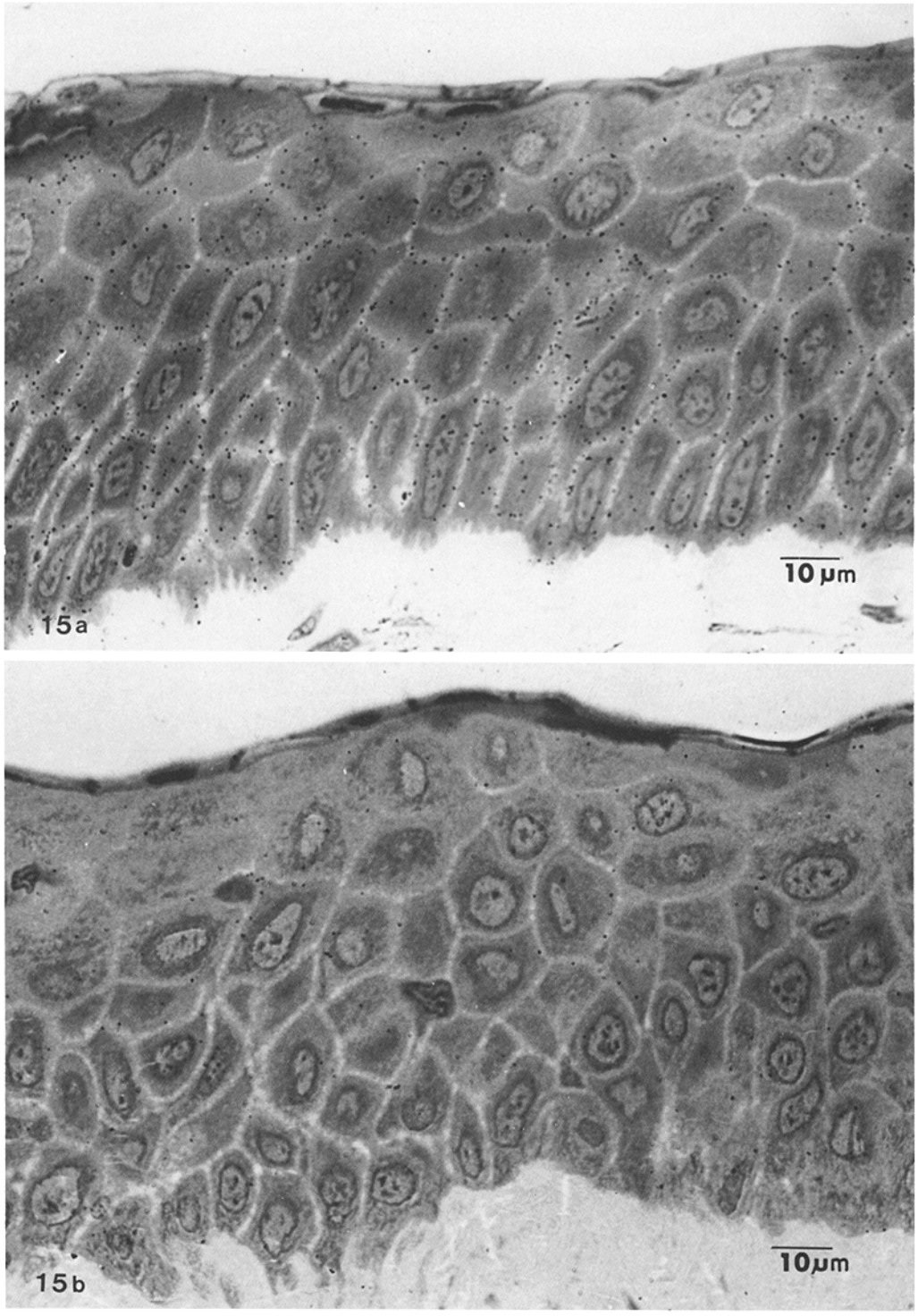

FIGURE 15 Radioautograph of two pieces of skin, from the same animal, incubated in 10^{-6} M [^{3}H]ouabain for 30 min followed by a 60-minute wash in ouabain-free Na^+-Ringer's. (*a*) Bathed in Na^+-Ringer's solution. (*b*) Bathed in 42 mM K^+-Ringer's solution. In Fig. 15*b* the reduction in grains associated with each layer is obvious. Notice that the morphology of the skin bathed in a 42 mM K^+-Ringer's is identical to that of the piece bathed in Na^+-Ringer's solution. 28-day exposure. (*a* and *b*) × 880.

as with treatment with 42 mM K^+, each cell layer was affected since the relative distribution was not significantly altered as compared to reoxygenated controls, even though ouabain binding was reduced by 55%.

It might be argued that inhibition of the pumps located in the spiny or germinal layer does not seriously affect the rate of active extrusion because the cells of the granular layer are responsible for most of the Na^+ transport, or that the cells in the outer layer may be able to maintain a high level of transport in response to an inhibition of pump sites farther along the pathway. This problem was investigated by exposing chamber-mounted skins to ouabain for 30 min, followed by a wash period, and then a continued incubation in ouabain-free Ringer's solution. After a 30-min exposure to 10^{-6} M ouabain, there was a slight effect on SCC (cf. Fig. 5). After the washout of unbound ouabain, the SCC on the ouabain-treated side declined continuously. 90 min post-washout, the SCC of the ouabain-treated side was inhibited by 36 ± 8% (n = 6) while the control side did not decline. Radioautographic analysis of skins treated in this manner showed that 92% of the grains were localized to the spiny and germinal layer (Fig. 10 D).

The final set of experiments was aimed at determining the distribution of ouabain-binding sites in skin where the Na^+ transport had been reduced to zero. For this purpose 10^{-5} M ouabain was added to one of a pair of mounted skins, while the other was exposed to 10^{-6} M ouabain. Incubation was continued until the SCC in the skin exposed to 10^{-5} M ouabain reached zero, and then the normal washout was conducted for each. Analysis of binding sites (Fig. 10 E) showed that, although the skins exposed to the higher concentration bound almost twice as much ouabain (Table II), the relative distribution of binding sites was essentially the same as in Fig. 10 A.

DISCUSSION

Localization of the Na^+ Pump

The results of this study support the following important conclusions: *a*) ouabain-binding sites, as revealed by radioautography of freeze-dried tissue, accurately reflect the distribution of Na^+-K^+-ATPase and, therefore, the sites of the Na^+-pump in the frog skin and *b*) all the living cell layers participate in the active transport step for Na^+ absorption across the skin.

As demonstrated by radioautography there is a significant number of grains associated with the inward facing membranes of all the living cell layers. The ouabain-binding sites associated with the cornified layer were not significantly different from background. All other layers had significantly more pump sites than background. This was the case whether the binding was expressed as the percentage in each layer or as the percent in 10 slices of equal area extending from the outer edge of the corneum to the base of the germinal layer.

Even though Na^+ pumps are distributed throughout the epithelium, the distribution is not even. The spiny and germinal layers account for the overwhelming majority of pump sites. When the grain distribution is expressed as the percent in each of 10 equivalent slices, numbered from outside edge to basal lamina, slices 5, 6, and 7 located in the spiny layer are each significantly greater in density than slices 1–4, 9, and 10 ($P < 0.02$). Thus, the middle portion of the skin, largely containing cells of the *stratum spinosum* (18), has the greatest number and density of Na^+-pump sites. The germinal layer also has a large fraction of the pumps. However, this figure is probably artificially high since the way in which we defined the zones for grain counting necessitated the inclusion of portions of cells of the spiny layer within the germinal layer.

The number of Na^+ pumps in the granular layer is also significantly greater than background. The results indicate, however, that the outer living cell layer of the frog skin, the reactive cell layer of Voûte and Ussing (47), does not have an exceptionally large fraction of the Na^+ pumps when compared to the other layers and is probably not the major site for active Na^+ extrusion in the frog skin.

The localization of pump sites in the deeper cell layers does not, by itself, indicate the actual pathway for the Na^+ actively transported across the epithelium. The cells in the germinal and spiny layers will eventually become cells of the granular layer, and it would seem logical for these cells to have developed an adequate number of pumps before this. However, these cells appear to be involved in Na^+ transport even before differentiation into the cells of the outer layer. This is substantiated by the fact that, after exposing the skin to 10^{-5} M ouabain for the time necessary to reduce the SCC to zero, the grain distribution was identical to that of skin exposed to 10^{-6} M. Thus, when all of the Na^+ pumps are inhibited by oua-

bain, the inner cell layers still exhibit the overwhelming majority of binding sites.

Specificity of [^{3}H]Ouabain Binding

The validity of the [^{3}H]ouabain radioautographic technique as a method for localizing the Na^+ pump depends on proof that: *a*) binding can be correlated with an inhibition of transport, *b*) ouabain reaches all available binding sites, and *c*) ouabain binding is specific for Na^+-K^+-ATPase. Baker and Willis (3) and Brading and Widdicombe (5) demonstrated a nonsaturable component of ouabain binding, unrelated to the effect of the glycoside on transport, which occurs at concentrations above 10^{-6} M. At ouabain concentrations below this level there is a saturable component of binding which demonstrates a strict correlation between amount of bound ouabain and inhibition of transport. We also found a nonsaturable component of ouabain binding in the frog skin that was detectable at concentrations above 10^{-5} M. Although no attempt was made to quantitatively correlate ouabain bound with inhibition of SCC, it is evident from Fig. 2 that there is a time-dependent correlation between ouabain concentration and degree of inhibition of SCC across the frog skin. The ouabain concentration that we employed, between 1.2 and 1.6 $\times$ 10^{-6} M, was low enough that binding to a nonsaturable component should not constitute a large proportion of the total amount bound while still sufficient to effectively inhibit SCC (Fig. 5).

Analysis of the data in Fig. 3 revealed that complete uptake by the saturable component of ouabain binding was achieved at ~1.55 pmol/mg wet weight. Skins exposed to 10^{-6} M ouabain never reached this value whether incubated in vials or mounted in chambers. This might be taken as evidence that ouabain, at this concentration, does not reach all the available binding sites. There are several reasons why this is probably not the case however. Analysis of [^{14}C]inulin distribution showed that this marker reached equilibrium in the extracellular space by 90 min. Since the incubations with ouabain were carried out for 120 min there was adequate time for this smaller molecule to diffuse throughout the extracellular space. Also, as mentioned in the results comparing binding with inhibition of transport by 10^{-5} vs. 10^{-6} M ouabain, the SCC in skins exposed to the higher concentrations does reach zero; yet, the distribution of [^{3}H]ouabain is identical to that in skins exposed to the lower concentration. This is strong evidence that ouabain even at 10^{-6} M reaches all the transport-related sites. Further evidence that all the pump sites are exposed to ouabain is shown in Fig. 12. Skins incubated for 90 min with [^{3}H]ouabain and frozen without washout of unbound label showed that ouabain had diffused throughout all the intercellular spaces.

The main criterion for determining the specificity of binding resides in manipulating the concentration of ligands that affect the binding of ouabain to Na-K-ATPase (31, 42). Specific binding requires Na^+, Mg^{++}, and ATP and is reduced by increasing the concentration of K^+ (36). Changing the concentration of these ligands also affects binding of ouabain to intact cells (2, 3, 20, 22, 32, 34). We were able to demonstrate the specificity of binding in the frog skin by either lowering the concentration of ATP in the cells or raising the K^+ concentration in the Ringer's solution bathing the tissue.

Although it is difficult to greatly reduce ATP concentrations in intact cells, an effective reduction can be achieved by incubating the cells in an anaerobic environment (21, 26). In experiments aimed at reducing ATP levels by incubation under anaerobic conditions, binding of ouabain in skins continuously exposed to anoxic conditions was reduced by 55%, in comparison to reoxygenated controls, and by 70% when compared to skins that had not undergone any anoxic period (Table II). The reduction in binding can be directly attributed to a reduction in ATP or to the fact that Na^+-pump activity is reduced in an anoxic environment. In either case the results indicate that ouabain binding has a high degree of specificity for the Na^+ pump in the frog skin.

Specificity of binding was also demonstrated by increasing the K^+ concentration in the Ringer's solution bathing the cells. Although K^+ reduces binding of ouabain to Na^+-K^+-ATPase preparations as well as to intact cells, the use of this technique as a rigorous test for specificity must be approached with caution. K^+ affects the rate of binding rather than causing a reduction of the maximal amount bound. Na^+-K^+-ATPase preparations, incubated for prolonged periods of time with ATP, Mg^{++}, Na^+, and K^+, eventually bind the same amount of ouabain as enzyme preparations incubated with ATP, Mg^{++}, and Na^+ without K^+ (1). This effect on rate of binding has also been demonstrated in intact cells (20, 28). As shown in Figs. 6 and 7 this was also the case for ouabain binding to frog skin. Raising the K^+ concentration

in the Ringer's solution bathing the frog skin reduced the rate of binding but had little effect on the maximal amount bound.

Therefore, when the amount of specific binding of ouabain is determined by manipulation of the K^+ concentration, the time of exposure to the glycoside is a critical factor. This is an especially important consideration in systems such as the frog skin where exposure of individual cells or cell layers to ouabain is not simultaneous. Increasing the incubation time to assure adequate exposure of all cells to ouabain, will mask the effect of K^+ on specific binding sites. Thus the amount of ouabain bound to intact cells in the presence of a high K^+ medium, when compared to the amount bound in a low K^+ medium, should not be considered a nonspecific component of binding but can actually still be specific binding to Na^+-K^+-ATPase sites.

These tests of specificity, along with the evidence that ouabain can completely inhibit Na^+ transport across the frog skin, provide adequate proof that [^{3}H]ouabain is a higly specific and physiologically relevant marker for the Na^+ pump.

Relevance to Models of Na^+ Transport

The radioautographic results obtained with [^{3}H]ouabain in the frog skin provide a quantitative morphological localization of Na^+-K^+-ATPase in this tissue that is correlated with inhibition of the Na^+ pump. It should be emphasized that, although these results with [^{3}H]ouabain are in some ways similar to those obtained with a cytochemical method for localization of Mg^{++}-ATPase (19), there are some important differences. First, we found no binding of ouabain to the outer membrane of the outermost living cell layer nor to the cells in the cornified layer, whereas the ATPase reaction product had been localized there (19). Second, binding of ouabain to the skin was altered by changing the concentration of ligands that effect binding of this cardiac glycoside to Na^+-K^+-ATPase enzyme preparations. Conversely, the cytochemical reaction product was insensitive to changes in the incubation medium that alter Na^+-K^+-ATPase activity (such as changes in the Na^+ and K^+ concentrations or the addition of ouabain). These important distinctions between the localization of a Mg^{++}-ATPase and the actual sites of Na^+-K^+-ATPase are further substantiated by Hokin et al. (23) who, in an attempt to purify Na^+-K^+-ATPase, were able to remove almost all Mg^{++}-ATPase activity. These facts demonstrate that the cytochemical localization of Mg^{++}-ATPase by the procedure of Wachstein and Meisel (50) probably is not related to the localization of the Na^+-K^+-ATPase (43).

The obvious involvement of all the living cell layers in the active transport of Na^+ across the frog skin is in general agreement with the model proposed by Ussing and Windhager (45). In that model the major site for the Na^+ pump was postulated to be at the innermost cell membrane. We propose a model that makes a quantitative distinction regarding the distribution of pumps with the major activity occurring in the cell layers deep to the outer living cell layer. As depicted in Fig. 16, all of the Na^+ to be actively transported enters the epithelium across the outer membrane of the outermost living cell layer (the only living cell membrane that had no ouabain-binding sites). A portion of this is actively extruded into the intercellular space by this first layer of cells. However, a considerably larger portion of the Na^+ passes through low resistance intercellular connections to the cells of the deeper layers. Most of the Na^+ that enters the frog skin is then actively extruded by cells in the spiny and germinal layers. The interiors of all the living cells are connected by low resistance intercellular connections which facilitate the passage of Na^+. The presence of specialized junctional areas throughout the epithelium of the frog skin, termed maculae and fasciae occludentes, has been described by Farquhar and Palade (18). These junctions are morphologically similar to the nexus, which is thought to be an area of low resistance coupling between excitable cells such as smooth muscle and myocardial cells (11).

This proposed model is compatible with the other principal function of the skin, which is protection.The frog skin goes through a molt cycle which results in the successive replacement of each layer with cells from the next deeper layer. The outermost layer is composed of dead, cornified cells. Although they have no active role in the reabsorption of ions and water, these cells probably serve a protective function against both physical trauma and dehydration. The outer living cell layer, also called the replacement layer (6), is composed of cells that will become the next cornified layer. That most of the Na^+ pumps are located deep in the epithelium assures continuity of the NaCl reabsorptive activity even while a whole layer of cells (the outermost living cell layer) is becoming cornified and losing its ability to act as a selective permeability barrier. This proposed scheme also predicts, as does the model proposed

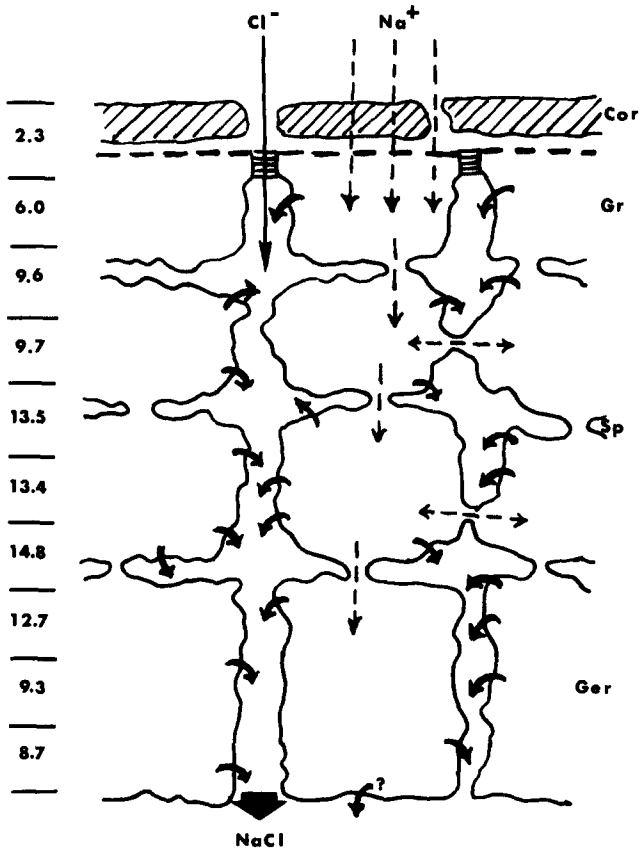

FIGURE 16 A model for active Na^+ transport across the frog skin which is based on the findings presented in this study. Na^+ is shown diffusing through or between the cells of the cornified layer (*Cor*) and then entering the granular layer (*Gr*) across the outward facing membrane which is selectively permeable to Na^+ (broken line). Dashed arrows indicate passive movement of Na^+. Once the Na^+ enters the epithelium, a portion of it is actively pumped (large solid arrows) across the inward-facing membrane of the first living cell layer while most of it diffuses through intercellular connections to the other layers and then is actively extruded into the extracellular space. The solid lines delineating the boundaries of the inward-facing cell membrane indicate that these are barriers selectively permeable to K^+ and impermeable to Na^+. The question mark next to the pump arrow in the basal membrane of the germinal layer indicates that we were unable to determine whether this membrane was a major site for the Na^+ pump. Cl^- (solid arrow) is depicted to move passively across the epithelium by a paracellular pathway. The emergent absorbate (large arrowhead) is a neutral NaCl solution. Numbers to the left of the model indicate the distribution of pumps (by percent) in 10 slices of the epithelium (see Fig. 11) after correction for background. The location of the pumps within the model reflects this distribution. Sp = spiny layer (2 cells thick), Ger = germinal layer.

by Farquhar and Palade (19), that, as a cell progressively differentiates from a germinal to a cornified cell, there is a significant modification of the plasmalemma so that the eventual outward facing portion of the membrane no longer has Na^+-pump sites or is permeable to K^+ and has become selectively permeable to Na^+.

In conclusion, we propose a mode depicting the pathway for the movement of Na^+ across the frog skin that includes all the inward-facing (serosal) membranes of the living cells as the site of the Na^+ pump. Furthermore, the cell layers deep to the outermost living layer have the overwhelming majority of pump sites. This scheme is in general agreement with measurements of the potential profile (45) and electrical impedance (38) of the skin and is compatible with consideration of the molt cycle of this epithelium.

We would like to gratefully acknowledge the technical assistance of Bonnie P. Lord and Barbara F. Reiner.

This research was supported by grants U. S. Public Health Service HE 06664 and AM 17372, National Science Foundation GB-42029, and RR-05417 Biomedical Research Support Grant awarded to Temple University. J. W. Mills is a fellow of the Pharmaceutical Manufacturer's Association Foundation, Inc. S. A. Ernst has a Career Development Award no. 5K04GM000-72 from the National Institutes of Health. A preliminary report of this work has already appeared (33).

Received for publication 14 July 1976, and in revised form 8 November 1976.

REFERENCES

1. ALLEN, J. C., and A. SCHWARTZ. 1970. Effects of potassium, temperature and time on ouabain interaction with the cardiac Na^+-K^+-ATPase. Further evidence supporting an allosteric site. *J. Mol. Cell. Cardiol.* **1**:39–45.
2. BAKER, P. F., and J. S. WILLIS. 1970. Potassium ions and the binding of cardiac glycosides to mammalian cells. *Nature (Lond.).* **226**:521–523.
3. BAKER, P. F., and J. S. WILLIS. 1972. Binding of the cardiac glycoside ouabain to intact cells. *J. Physiol. (Lond.).* **224**:441–462.
4. BELANGER, L. F. 1961. Staining processed radioautographs. *Stain Tech.* **36**:313–317.
5. BRADING, A. F., and J. H. WIDDICOMBE. 1974. An estimate of sodium potassium pump activity and the number of pump sites in the smooth muscle of the guinea pig *taenia coli* using (^{3}H) ouabain. *J. Physiol. (Lond.).* **238**:235–249.
6. BUDTZ, P. E., and L. O. LARSON. 1973. Structure of the toad epidermis during the moult cycle. I. Light microscopic observations in *Bufo bufo* (L). *Z. Zellforsch Mikrosk. Anat.* **144**:353–368.
7. CARASSO, N., P. FAVARD, S. JARD, and R. M. RAJERISON. 1971. The isolated frog skin epithelium. I. Preparation and general structure in different physiological states. *J. Microsc. (Paris).* **10**:315–330.
8. CEREIJIDO, M., and C. A. ROTUNNO. 1968. Fluxes and distribution of sodium in frog skin. A new model. *J. Gen. Physiol. (Suppl.).* **51**:280–289s.
9. CIVAN, M. M., and R. E. HOFFMAN. 1971. Effect of aldosterone on electrical resistance of toad bladder. *Am. J. Physiol.* **220**:324–328.
10. CLELAND, W. W. 1967. The statistical analysis of enzyme kinetic data. *In* Advances in Enzymology. F. F. Nord, editor. John Wiley & Sons, Inc., New York. **29**:1–32.
11. DEWEY, M. M., and L. BARR. 1964. A study of the structure and distribution of the nexus. *J. Cell Biol.* **23**:553–585.
12. DORGE, A., K. GEHRING, W. NAGEL, and K. THURAU. 1974. Localization of sodium in frog skin by electron microprobe analysis. *Arch. Pharmakol. Exp. Pathol.* **281**:271–280.
13. DUNHAM, P. B., and R. B. GUNN. 1972. Adenosine triphosphatase and active cation transport in red blood cell membranes. *Arch. Intern. Med.* **129**:241–247.
14. ERNST, S. A., C. C. GOERTEMILLIER, JR., and R. A. ELLIS. 1967. The effect of salt regimens on the development of (Na^+-K^+)-dependent ATPase activity during growth of salt glands of domestic ducklings. *Biochem. Biophys. Acta.* **135**:682–691.
15. ERNST, S. A., and C. W. PHILPOTT. 1970. Preservation of Na^+-K^+-activated and Mg^+-activated adenosine triphosphatase activities of avian salt gland and teleost gill with formaldehyde as fixative. *J. Histochem. Cytochem.* **18**:251–263.
16. ERNST, S. A. 1972. Transport adenosine triphosphatase cytochemistry. I. Biochemical characterization of a cytochemical medium for the ultrastructural localization of ouabain-sensitive, potassium-dependent phosphatase activity in the avian salt gland. *J. Histochem. Cytochem.* **20**:13–22.
17. ERNST, S. A. 1972. Transport adenosine triphosphatase cytochemistry. II. Cytochemical localization of ouabain-sensitive, potassium-dependent phosphatase activity in the secretory epithelium of the avian salt gland. *J. Histochem. Cytochem.* **20**:23–38.
18. FARQUHAR, M. G., and G. E. PALADE. 1965. Cell junctions in amphibian skin. *J. Cell Biol.* **26**:263–291.
19. FARQUHAR, M. G., and G. E. PALADE. 1966. Adenosine triphosphatase localization in amphibian epidermis. *J. Cell Biol.* **30**:359–379.
20. GARDNER, J. D., and T. P. CONLON. 1972. The effect of sodium and potassium on ouabain binding by human erythrocytes. *J. Gen. Physiol.* **60**:609–629.
21. HANDLER, J. S., A. S. PRESTON, and J. ROGULSKI. 1960. Control of glycogenolysis in toad's urinary bladder. *J. Biol. Chem.* **243**:1376–1383.
22. HOFFMAN, J. F. 1969. The interaction between tritiated ouabain and the Na^+-K^+-pump in red blood cells. *J. Gen. Physiol.* **54**(Suppl.):343–350s.
23. HOKIN, L. E., J. L. DAHL, J. D. DUPREE, J. F. DIXON, J. F. HACKNEY, and J. F. PERDUE. 1973. Studies on the characterization of the sodium-potassium transport adenosine triphosphatase. X. Purification of the enzyme from the rectal gland of *Squalus acanthas*. *J. Biol. Chem.* **248**:2593–2605.
24. KOEFOED-JOHNSEN, V. 1957. The effect of g-strophanthin (ouabain) on the active transport of sodium through the isolated frog skin. *Acta. Physiol. Scand. Suppl.* **42**:145.
25. KOEFOED-JOHNSEN, V., and H. H. USSING. 1958. The nature of the frog skin potential. *Acta Physiol. Scand.* **42**:298–308.

26. KRISTENSEN, P., and A. SCHOUSBOE. 1969. The influence of anaerobic conditions on sodium transport and adenine nucleotide levels in the isolated skin of the frog *Rana temporaria*. *Biochim. Biophys. Acta.* **173:**206–212.
27. KYTE, J. 1972. The titration of the cardiac glycoside binding sites of the (Na^+-K^+) adenosine triphosphatase. *J. Biol. Chem.* **247:**7634–7641.
28. LANDOWNE, D., and J. M. RITCHIE. 1970. The binding of tritiated ouabain to mammalian nonmyelinated nerve fibres. *J. Physiol. (Lond.).* **207:**529–537.
29. LINDENMAYER, G. W., and A. SCHWARTZ. 1970. Conformational changes induced in Na^+-K^+-ATPase by ouabain through a K^+ sensitive reduction: Kinetic and spectroscopic studies. *Arch. Biochem. Biophys.* **140:**371–378.
30. MATSUI, H., and A. SCHWARTZ. 1967. ATP-dependent binding of ^{3}H-digoxin to a Na^+-K^+-ATPase from cardiac muscle. *Fed. Proc.* **26:**398.
31. MATSUI, H., and A. SCHWARTZ. 1968. Mechanism of cardiac glycoside inhibition of the Na^+-K^+-dependent ATPase from cardiac tissue. *Biochim. Biophys. Acta.* **151:**655–663.
32. MILLS, J. W., and S. A. ERNST. 1975. Localization of sodium pump sites in frog urinary bladder. *Biochim. Biophys. Acta.* **375:**268–273.
33. MILLS, J. W., and S. A. ERNST. 1975. Localization of ^{3}H-ouabain binding sites in frog skin. *J. Cell Biol.* **67 (2,** Pt. 2)**:**287 a. (Abstr.)
34. QUINTON, P. M., E. M. WRIGHT, and J. MCD. TORMEY. 1973. Localization of sodium pumps in the choroid plexus epithelium. *J. Cell Biol.* **58:**724–730.
35. SACHS, J. R., P. B. DUNHAM, D. L. KROPP, J. C. ELLORY, and F. HOFFMAN. 1974. Interaction of HK and LK goat red blood cells with ouabain. *J. Gen. Physiol.* **64:**536–550.
36. SCHWARTZ, A., G. E. LINDENMAYER, and J. C. ALLEN. 1975. The sodium-potassium adenosine triphosphatase: pharmacological, physiological and biochemical aspects. *Pharmacol. Rev.* **27:**3–134.
37. SKOU, J. C. 1965. Enzymatic basis for active transport of Na^+ and K^+ across cell membranes. *Physiol. Rev.* **45:**596–617.
38. SMITH, P. G. 1971. The low frequency electrical impedence of the isolated frog skin. *Acta. Physiol. Scand.* **81:**355–366.
39. SPURR, A. R. 1969. A low viscosity epoxy resin embedding medium for electron microscopy. *J. Ultrastruct. Res.* **26:**31–43.
40. STIRLING, C. E. 1972. Radioautographic localization of sodium pump sites in rabbit intestine. *J. Cell Biol.* **53:**704–714.
41. STIRLING, C. E. 1976. High resolution autoradiography of ^{3}H-ouabain binding in salt transporting epithelia. *J. Microsc. (Oxf.).* **106:**145–158.
42. TOBIN, T., and A. K. SEN. 1970. Stability and ligand sensitivity of (^{3}H) ouabain binding to (Na^+ + K^+)-ATPase. *Biochim. Biophys. Acta.* **198:**120–131.
43. TORMEY, J. MCD. 1966. Significance of the histochemical demonstration of ATPase in epithelia noted for active transport. *Nature (Lond.).* **210:**820–822.
44. USSING, H. H., and K. ZERAHN. 1951. Active transport of sodium as the source of electric current in short-circuited isolated frog skin. *Acta. Physiol. Scand.* **23:**110–127.
45. USSING, H. H., and E. E. WINDHAGER. 1964. Nature of shunt path and active sodium transport path through frog skin epithelium. *Acta. Physiol. Scand.* **61:**484–504.
46. USSING, H. H., T. U. L. BIBER, and N. S. BRICKER. 1965. Exposure of the isolated frog skin through potassium concentrations at the internal surface. II. Changes in epithelial cell volume, resistance, and response to antidiuretic hormone. *J. Gen. Physiol.* **48:**425–433.
47. VOÛTE, C. L., and H. H. USSING. 1968. Some morphological aspects of active sodium transport. The epithelium of the frog skin. *J. Cell Biol.* **36:**625–638.
48. VOÛTE, C. L., and S. HANNI. 1973. Relation between structure and function in frog skin. *In* Transport Mechanisms in Epithelia. Proceedings The Alfred Benzon Symposium. V. H. H. Ussing and N. A. Thorn, editors. Munksgaard, Copenhagen. 86–93.
49. VOÛTE, C. L., K. MØLLGARD, and H. H. USSING. 1975. Quantitative relationship between active sodium transport, expansion of endoplasmic reticulum and specialized vacuoles ("scalloped sacs") in the outermost living cell layer of the frog skin epithelium (Rana temporaria). *J. Membr. Biol.* **21:**273–289.
50. WACHSTEIN, M., and E. MEISEL. 1957. Histochemistry of hepatic phosphatase at a physiologic pH. With special reference to the demonstration of bile canaliculi. *Am. J. Clin. Pathol.* **27:**13–23.